Journal of Neuroimaging

WILEY

JOURNAL OF NEUROIMAGING
THE OFFICIAL JOURNAL OF THE AMERICAN SOCIETY OF NEUROIMAGING

CLINICAL INVESTIGATIVE STUDY OPEN ACCESS

Poststroke Translocator Protein Expression Dynamics and Correlations to Chronic Infarction: A [123I]-CLINDE-SPECT Study

Per Jensen[1,2] | Brice Ozenne[1,3] | Per Meden[4] | Ling Feng[1] | Gerda Thomsen[1] | Lars Knudsen[1] | Henrik Steglich-Arnholm[5] | Kirsten Møller[6,7] | Carsten Thomsen[8] | Claus Svarer[1] | Vincent Beliveau[1] | Jens Mikkelsen[1,9] | Gitte Knudsen[1,9] | Lars H Pinborg[1,2]

[1]Neurobiology Research Unit, Rigshospitalet, University of Copenhagen, Copenhagen, Denmark | [2]Epilepsy Clinic, Rigshospitalet, University of Copenhagen, Copenhagen, Denmark | [3]Department of Public Health, Section of Biostatistics, University of Copenhagen, Copenhagen, Denmark | [4]Department of Neurology, Bispebjerg Hospital, University of Copenhagen, Copenhagen, Denmark | [5]Department of Neurology, Rigshospitalet, University of Copenhagen, Copenhagen, Denmark | [6]Department of Clinical Medicine, Faculty of Health and Medical Sciences, University of Copenhagen, Copenhagen, Denmark | [7]Department of Neuroanaesthesiology, Rigshospitalet, University of Copenhagen, Copenhagen, Denmark | [8]Department of Radiology, Rigshospitalet, University of Copenhagen, Copenhagen, Denmark | [9]Faculty of Health and Medicine, University of Copenhagen, Copenhagen, Denmark

Correspondence: Lars H Pinborg (lars.pinborg@nru.dk)

Received: 19 April 2024 | **Revised:** 15 December 2024 | **Accepted:** 16 December 2024

Funding: This work was financially supported by the European Union's seventh framework programme the grant agreement no. HEALTH-F2-2011-278850 (INMiND), the Danish Council for Independent Research, the Research Committee of Rigshospitalet, and Desirée and Niels Yde ś foundation.

Keywords: MRI | neuroinflammation | SPECT | stroke | translocator protein

ABSTRACT

Background and Purpose: This study aims to investigate the longitudinal changes in translocator protein (TSPO) following stroke in different brain regions and potential associations with chronic brain infarction.

Methods: Twelve patients underwent SPECT using the TSPO tracer 6-Chloro-2-(4′-123I-Iodophenyl)-3-(*N*,*N*-Diethyl)-Imidazo[1,2-a]Pyridine-3-Acetamide, as well as structural MRI, at 10, 41, and 128 days (median) after ischemic infarction in the middle cerebral artery. TSPO expression was measured in lesional (MRI lesion and SPECT lesion), connected (pons and ipsilesional thalamus), and nonconnected (ipsilesional cerebellum and contralesional occipital cortex) regions. Correlations were explored between the volume of chronic infarction and TSPO expression in nonconnected regions of interest (ROIs) at 128 days

Results: Throughout the study period, TSPO levels decreased by 24%–33% in lesional ROIs, while levels increased in connected ROIs by 35%–69% and in nonconnected ROIs by 53%–77%. At 128 days poststroke, TSPO expression in ipsilesional cerebellum positively correlated with chronic infarction volume ($p = 0.002$, $r^2 = 0.72$).

Conclusions: This study expands the current knowledge of spatial and temporal TSPO expression in humans by quantifying TSPO changes in lesional, connected, and nonconnected brain regions at three time points after cerebral infarction as well as correlating late-stage TSPO upregulation and chronic infarction volume.

1 | Introduction

In the aftermath of an acute ischemic stroke, the neuroinflammatory response may persist for several months. Modulating this response could lead to improved functional outcomes, but this necessitates a detailed comprehension of the temporal and spatial dynamics of poststroke neuroinflammation [1]. Following stroke, the inflammatory response involves microglial activation, releasing proinflammatory cytokines that may contribute to tissue damage [2]. Conversely, microglia can also transition into neuroprotective phenotypes, reinstating tissue homeostasis and facilitating reorganization of synapses during the rehabilitation phase [3, 4].

The SPECT tracer 6-Chloro-2-(4'-123I-Iodophenyl)-3-(*N*,*N*-Diethyl)-Imidazo[1,2-a]Pyridine-3-Acetamide (^{123}I-CLINDE) targets translocator protein (TSPO), which is upregulated in the mitochondria of microglia cells, as a response to tissue damage, in the process of transitioning from resting to activated phenotypes as well as other immunocompetent cells in the brain (i.e., activated astrocytes and migrating peripheral macrophages) [5]. Thus, ^{123}I-CLINDE SPECT is a tool for imaging studies of neuroinflammation.

Previous imaging studies on TSPO in ischemic stroke patients have found minimal upregulation within the first 72 h, followed by upregulation in and around the lesion as well as in efferent fiber tracts such as the pyramidal tract in the pons [6, 7]. In succession, ipsilesional thalamus TSPO upregulation has been observed at 4–6 weeks, and in the contralesional thalamus at 128 days [8–10]. Although several previous studies have carried out consecutive TSPO imaging protocols on stroke patients, it is worth mentioning that only the study conducted by Thiel et al. undertook statistical analysis to evaluate temporal TSPO changes. Notably, their longitudinal analysis was specifically focused on the lesion, where a statistically significant longitudinal decrease in TSPO expression was demonstrated, and on the pons, where no statistically significant temporal TSPO alterations were observed [10]. Thus, detailed longitudinal quantitative measurements focusing on both spatial and temporal aspects of poststroke TSPO expression in humans are warranted.

In this study, patients with a first-ever infarction in the middle cerebral artery (MCA) underwent ^{123}I-CLINDE SPECT and MRI at three successive time points after the onset of stroke. The regions of interest (ROIs) were categorized into three groups based on their relation to the infarct as defined below: lesional, connected, and nonconnected.

Lesional ROIs were defined on T2-weighted MRI (MRI lesion ROI) and ^{123}I-CLINDE SPECT measures (SPECT lesion ROI). The current study aims to investigate the relationship between the initial site of TSPO upregulation after stroke and the lesion as depicted on T2-weighted MRI, as the overlap between the two is only partial and warrants further investigation [11].

Connected ROIs were defined as anatomical brain regions with connecting efferent fiber tracts from the infarct, specifically the ipsilesional thalamus and the pons. While thalamic TSPO upregulation after stroke has been previously reported in humans, it has not been quantitatively studied [9]. Our hypotheses were that both connected ROIs would demonstrate a temporal increase in TSPO.

The ipsilesional cerebellum and contralesional occipital cortex were defined as nonconnected ROIs and, to our knowledge, have not been studied longitudinally in human stroke patients before. The use of two-tissue compartmental (2-TCM) modeling with arterial input allowed us to explore these regions without the need for a brain reference region, and the longitudinal design enabled us to detect subtle temporal changes in TSPO [12]. Without apparent functional or structural association with the site of the infarct, TSPO changes in nonconnected ROIs may reflect a broader poststroke neuroinflammatory response. The previous assumption that TSPO changes in nonconnected ROIs are unaffected by stroke and only represent non-specific binding has been challenged by TSPO imaging studies of other neurological conditions such as traumatic brain injury and multiple sclerosis. These studies have shown diffuse brain TSPO increases that correlate with disease progression or functional outcome [2, 13, 14]. Our hypothesis was that the nonconnected ROIs would show a longitudinal increase in TSPO. Additionally, we hypothesized that late-stage TSPO measurements in these regions would positively correlate with the volume of chronic infarction.

2 | Methods

2.1 | Patient Inclusion and Genotyping

The study protocol was approved by the ethical committee of the Copenhagen Capital Region (H-2-2010-086 amendment 39319). All subjects provided written informed consent. Fourteen stroke patients with a first-ever infarction in the MCA territory and impairment of the contralesional upper extremity were included within the first week after onset. Two of the patients were unable to complete the first SPECT scan session and were excluded from the study. The remaining 12 patients were scanned consecutively three times at 10 [7; 15], 41 [37; 44], and 128 [101; 157] days after stroke. All subjects were genotyped for the rs6971 polymorphism to determine TSPO binder status, as previously described [12, 15].

2.2 | SPECT Scanning and Blood Sampling

SPECT and MRI images were acquired at the Copenhagen University Hospital. Ninety-minute dynamic ^{123}I-CLINDE SPECT scans were performed with a triple-head IRIX camera (Philips Medical). Arterial blood samples were drawn manually during SPECT scans to determine radioactivity in plasma and whole blood at 21 time points, with metabolite analysis performed using radio-high-performance liquid chromatography (radio-HPLC) at eight time points. The SPECT scanning and blood sampling protocol were previously described [12]. Furthermore, radioligand purity was measured for each batch of ^{123}I-CLINDE, and trapping efficiency of the HPLC column (plasma control) was determined twice for each blood sample batch by spiking water and blank plasma with ^{123}I-CLINDE.

2.3 | Structural MRI

Three-dimensional T1- and T2-weighted MRI, as well as fluid-attenuated inversion recovery (FLAIR), was performed within 24 h of the corresponding ^{123}I-CLINDE SPECT scan. Voxel size was 1 × 1 × 1 mm for both T1 and T2 images and 0.67 × 0.67 × 1.3 mm for FLAIR images. MRI was performed using a 3-T Prisma scanner (Siemens).

2.4 | ROIs and Image Processing

Six ROIs were delineated using different methods: automatic, semiautomatic, and manual delineation. After delineation, the regions were classified into three groups as lesional (MRI lesion and SPECT lesion), connected (pons, ipsilesional thalamus), and nonconnected (ipsilesional cerebellum, contralesional occipital cortex).

The SPECT lesion ROIs were delineated on the SPECT image semiautomatically by making an isocontour with a value above 1.5 times the mean cerebellar ^{123}I-CLINDE uptake as previously defined [16]. The MRI lesion ROIs were manually delineated in T2-weighted images on the first scan, based on the hyperintensity signal. Consecutively, the MRI and SPECT lesion ROIs were co-registered to the second and third scan (Figure 1). The overlap percentage of the SPECT lesion with the MRI lesion was defined as the common volume of MRI and SPECT lesion ROIs divided by the volume of the MRI lesion ROI. The volume of chronic infarction was quantified at 128 days poststroke by segmenting the lesions on FLAIR MRI and estimating the volume using ITK-SNAP software (v.4.2.0, Philadelphia, Pennsylvania, www.itksnap.org) [17].

Connected and nonconnected ROIs were automatically delineated in MRI scans using probability maps and a data processing pipeline as described previously [18].

All preprocessing was performed using Matlab (v.2013a, MathWorks Inc, Natick, Massachusetts, http://www.mathworks.com). The binding of ^{123}I-CLINDE to TSPO was estimated as distribution volume (V_T) using a 2-TCM model with arterial input as described previously [12].

2.5 | Statistical Analysis

To test the hypotheses concerning the temporal evolution of TSPO measures in the examined ROIs, we performed paired *t*-tests of the ^{123}I-CLINDE SPECT V_T at Day 10 versus Day 41 as well as Day 10 versus Day 128. Since only two patients were mixed-affinity binders (MABs), the genetic effect could not be estimated based on our data. By performing a paired *t*-test on the percentage difference between scans, we removed time-invariant genotype effects. In contrast to repeated measures ANOVA, the paired *t*-test offers greater flexibility by accommodating heteroscedasticity (variance changes over time) and enables an exclusive focus on comparisons derived from a baseline reference. The *p*-values underwent adjustment for multiple comparisons using the single step Dunnett's procedure, as specified in Section 7.1 of the referenced manuscript [19].

Linear Pearson correlations were conducted on the 10 high-affinity binder (HAB) patients to assess the relationship between chronic infarction volume and ^{123}I-CLINDE SPECT V_Ts in the nonconnected ipsilesional cerebellum at scan 3.

The analysis and graphical presentation were performed using the R software (v.2023, R core team, R Foundation for Statistical Computing, Vienna, Austria, https://www.R-project.org/). Results are given as median [range] unless specified otherwise.

3 | Results

3.1 | Patients

Twelve patients who experienced a first-ever infarction in the MCA territory were included in the final analysis of this study. The stroke patient group consisted of six females and sex males, with an average age of 60.7 [41.7; 66.7] years. Genotyping identified 10 individuals as HABs and two as MABs. No low-affinity binders were identified. The three consecutive scan times following stroke were 10 [7; 15] days for scan 1, 41 [35; 46] days for scan 2, and 128 [101; 157] days for scan 3. The injected dose of ^{123}I-CLINDE per scan was 116.7 [103.5; 137.0] MBq. For detailed patient data, please refer to Tables 1 and 2.

3.2 | TSPO Expression

The expression of TSPO exhibited considerable interpatient heterogeneity in both temporal and spatial aspects. This heterogeneity was particularly prominent in the lesional ROIs of the initial scans, with substantial variations observed in ROI sizes and ^{123}I-CLINDE SPECT V_Ts between patients. Table 3 provides the mean V_Ts for the 10 HAB patients, and Table 4 provides the longitudinal TSPO changes for all 12 patients. Figure 1 showcases the ^{123}I-CLINDE SPECT and MRI images, while the temporal evolution of ^{123}I-CLINDE expression is visually represented in Figures 2 and 3.

3.3 | Lesional ROIs

In the MRI lesion ROI, the ^{123}I-CLINDE SPECT V_T decrease of 17.0% between Day 10 and Day 41 was not significant ($p = 0.147$); however, ^{123}I-CLINDE SPECT V_T decreased significantly between Day 1 and Day 128 by 32.8% ($p < 0.001$).

For the SPECT lesion ROI, the mean ^{123}I-CLINDE SPECT V_T decreased by 17.4% ($p = 0.045$) between Day 10 and Day 41 and by 23.8% ($p = 0.017$) between Day 10 and Day 128.

3.4 | Connected ROIs

In the ipsilesional thalamus, ^{123}I-CLINDE SPECT V_T increases by 13.5% between Day 10 and Day 41 and 34.6% between Day 10 and Day 128 were not significant when corrected for multiple comparisons ($p = 0.456$ and $p = 0.157$). In the pons, ^{123}I-CLINDE SPECT V_Ts increased significantly by 46.2% ($p = 0.002$) between Day 10 and Day 41 and 68.8% ($p = 0.002$) between Day 10 and Day 128.

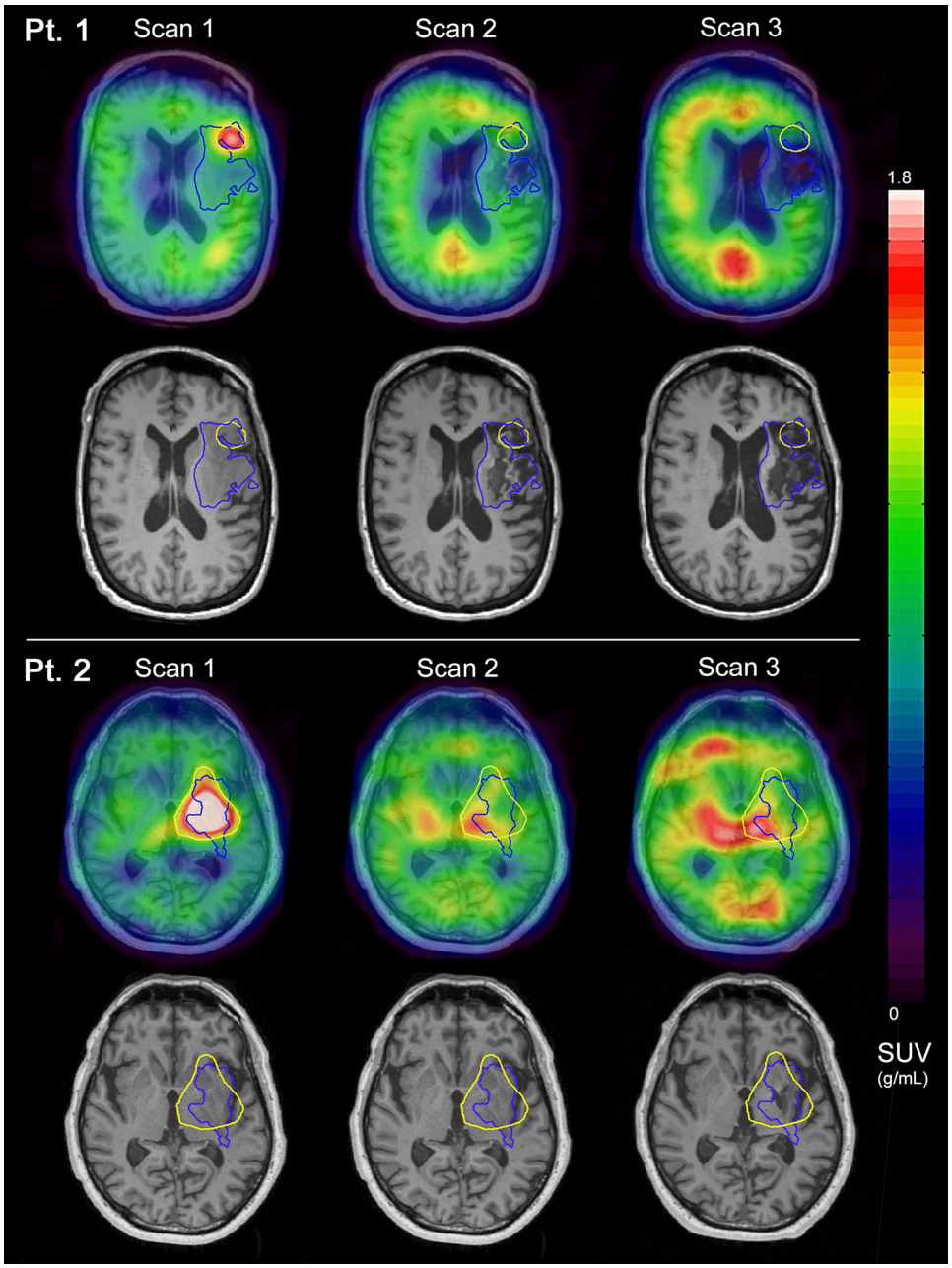

FIGURE 1 | ^{123}I-CLINDE SPECT and structural MRI in stroke patients. The figure displays ^{123}I-CLINDE SPECT and T1-weighted MRI in patient number 1 and 2 scanned longitudinally three times after infarction in the left middle cerebral artery. SPECT images were normalized by bodyweight and injected ^{123}I-CLINDE dose. Yellow regions of interest (ROIs) depict the lesional SPECT upregulation at scan 1, and blue ROIs depict the structural lesion delineated on T2-weighted MRI (not shown) at scan 1. Patients (Pt.) 1 and 2 underwent imaging at Day 10 following stroke. SUV, standardized uptake value.

3.5 | Nonconnected ROIs

In the ipsilesional cerebellum, there was a nonsignificant increase of 58.4% in ^{123}I-CLINDE SPECT V_T between Day 10 and Day 41 ($p = 0.087$). However, a significant increase of 77.0% ($p = 0.009$) was observed between Day 10 and Day 128.

The contralesional occipital cortex exhibited a V_T increase of 33.6% (p = 0.043) between Day 10 and Day 41 and 53.0% (p = 0.005) between Day 10 and Day 128.

3.6 | Lesion ROI Volume Overlap and Chronic Infarction

The measured volume of the SPECT lesion ROIs was 48.6 mL [7.1; 121.2], while the MRI lesion ROI had a volume of 40.4 mL [17.5; 76.1]. The SPECT lesion ROI overlapped the MRI lesion ROI by 68.7% [6.4; 90.4].

The volume of chronic infarction at 128 days poststroke was 17.7 mL [3.2; 60]. The volumes of chronic infarction are listed for the individual patients in Table 1.

TABLE 1 | Patients.

Patient no.	Days after stroke	Gender	Age at inclusion (years)	Translocator protein binder status	Injected 123I CLINDE (MBq)	Lesion volume at scan 1 (mL)	Chronic infarction volume at scan 3 (mL)
1	10	Female	52	HAB	108.9	76.1	
	38				113.4		
	101				103.1		60.0
2	10	Male	63	HAB	112.3	58.1	
	46				102.5		
	157				117.5		18.3
3	12	Male	57	HAB	135.7	31	
	40				114.8		
	130				126.8		15.7
4	15	Male	60	HAB	110.9	65.7	
	43				115.9		
	139				128.3		49.9
5	11	Female	42	HAB	127.3	75	
	39				114.7		
	131				108.9		17.7
6	9	Male	68	MAB	121.5	39.2	
	35				123.2		
	135				113		11.8
7	7	Female	72	HAB	118.9	17.5	
	41				117.7		
	126				108.3		12.9
8	13	Female	68	HAB	117.8	19.5	
	41				122.1		
	125				103.2		6.8
9	10	Female	59	MAB	137	41.7	
	37				117.4		
	121				122.1		28.0
10	13	Female	55	HAB	123.7	23.1	
	41				130.5		
	132				111.3		3.2
11	10	Male	61	HAB	113.6	52.8	
	38				112.8		
	122				114.4		19.5
12	10	Male	62	HAB	117.6	38.6	
	44				124.9		
	122				109.9		18.1

Note: The table displays data for the stroke patients.

Abbreviations: HAB, high-affinity binder; MAB, mixed-affinity binder; MBq, megabecquerel; no., number.

TABLE 2 | Clinical data.

Patients	Ischemic region	Cause of stroke (TOAST criteria)	Admission NIHHS	mRS at scan 3
Pt. 1	Left MCA	Other determined cause	20	1
Pt. 2	Left MCA	Other determined cause	18	2
Pt. 3	Left MCA	Large artery disease	8	2
Pt. 4	Left MCA	Large artery disease	19	2
Pt. 5	Right MCA	Other determined cause	20	1
Pt. 6	Right MCA	Other determined cause	22	2
Pt. 7	Right MCA	Cardioembolic	11	1
Pt. 8	Right MCA	Large artery disease	13	3
Pt. 9	Left MCA	Large artery disease	14	2
Pt. 10	Right MCA	Other determined cause	18	2
Pt. 11	Left MCA	Large artery disease	16	2
Pt. 12	Right MCA	Cardioembolic	17	3

Note: The table presents the affected artery, the cause of stroke according to the Trial of ORG 10172 in Acute Stroke Treatment (TOAST) classification, the admission National Institutes of Health Stroke Scale (NIHSS), and the modified Rankin Scale (mRS) score at scan 3.
Abbreviation: MCA, middle cerebral artery; Pt., patient.

TABLE 3 | Distribution volumes of translocator protein.

	Scan 1 (10 days)		Scan 2 (41 days)		Scan 3 (128 days)	
ROI	Mean V_T	Range	Mean V_T	Range	Mean V_T	Range
Lesional						
MRI lesion	9.3	[4.9; 13.9]	7.2	[5.6; 11.0]	6	[3.8; 7.0]
SPECT lesion	11.6	[8.1; 18.3]	9.1	[6.2; 12.7]	8.5	[5.9; 15.2]
Connected						
Ipsilesional thalamus	6.8	[5.6; 9.9]	7.6	[5.4; 11.0]	9.2	[5.2; 15.2]
Pons	5.8	[3.2; 7.7]	8.2	[5.0; 9.4]	10	[5.5; 16.4]
Nonconnected						
Ipsilesional cerebellum	3.8	[1.7; 5.1]	5.5	[4.1; 9.4]	6.5	[4.2; 12.3]
Contralesional Occ	4	[2.8; 5.3]	5.3	[4,1; 8.1]	6.1	[4.3; 9.1]

Note: The table lists the mean distribution volume (V_T) values and range for the 10 high-affinity TSPO binder patients.
Abbreviations: Occ, occipital cortex; ROI, region of interest.

3.7 | Correlations With Volume of Chronic Infarction

Investigation of the V_T of ^{123}I-CLINDE (HAB) in the ipsilesional cerebellum and the volume of chronic infarction at Day 128 revealed a positive linear correlation Pearson ($p = 0.001$, $r^2 = 0.78$). See Figure 4 for a scatterplot of the data.

4 | Discussion

This study has been undertaken within the scope of a doctoral project conducted at the University of Copenhagen's Neurobiology Research Unit, though the data remain unpublished in any scientific journal [20].

The present study provides insights into the temporal and spatial patterns of TSPO expression following stroke, exhibiting distinct characteristics among different ROI classes, namely lesional, connected, and nonconnected regions. Therefore, the subsequent discussion will focus on the neuroinflammatory response observed in these three distinct ROI classes.

Our results demonstrate a decline in ^{123}I-CLINDE SPECT V_T in both MRI and SPECT lesional ROIs during the study period. The findings are in general agreement with previous TSPO studies in human stroke. Ramsay et al. reported the first evidence of in vivo TSPO expression in a single stroke patient who underwent scans at 6, 13, and 20 days after infarction. Retention of [11C]-PK11195 surrounding the infarct border was discernible at Day 6, with further development of distinct areas of retention within

TABLE 4 | Longitudinal translocator protein changes.

Region of interest	Scan 1–2 (10 - 41 days)		Scan 1–3 (10 - 128 days)	
	Mean PD	*p*-value	Mean PD	*p*-value
Lesional				
MRI lesion	−17.00%	0.134	−32.80%	<0.001
SPECT lesion	−17.40%	0.039	−23.80%	0.014
Connected				
Ipsilesional thalamus	13.50%	0.435	34.60%	0.142
Pons	46.20%	0.001	68.50%	0.001
Nonconnected				
Ipsilesional cerebellum	58.40%	0.07	77.00%	0.008
Contralesional Occ	33.60%	0.037	53.00%	0.004

Note: The table lists the mean relative change in ^{123}I-CLINDE SPECT distribution volume (V_T) for all 12 patients as well as *p*-values adjusted for multiple comparisons.

Abbreviations: Occ, occipital cortex; PD, the percentage difference, calculated as the change in mean CLINDE V_T from scan 1 to either scan 2 or scan 3, divided by the mean CLINDE V_T at scan 1, then multiplied by 100.

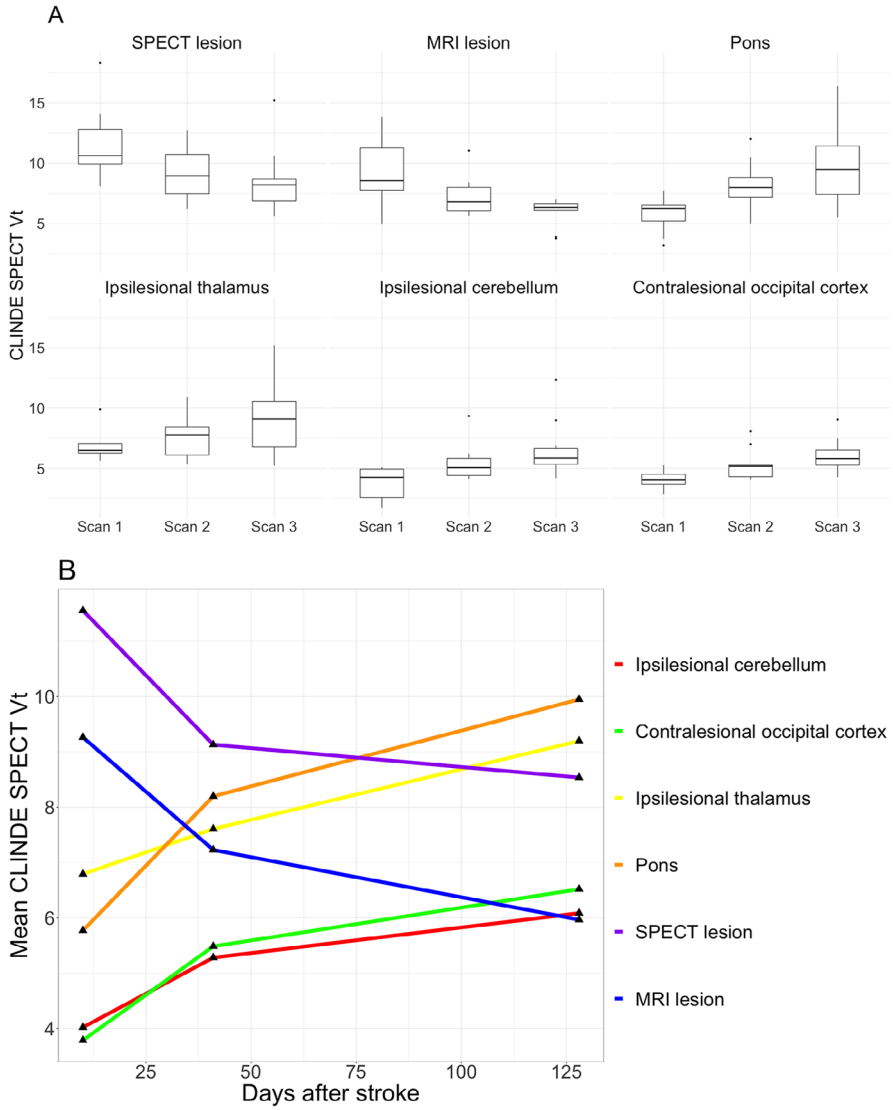

FIGURE 2 | Evolution of TSPO expression. Boxplots (A) and graphic illustration (B) of the temporal evolution of TSPO expression in 10 high affinity binder patients. Vt, distribution volume.

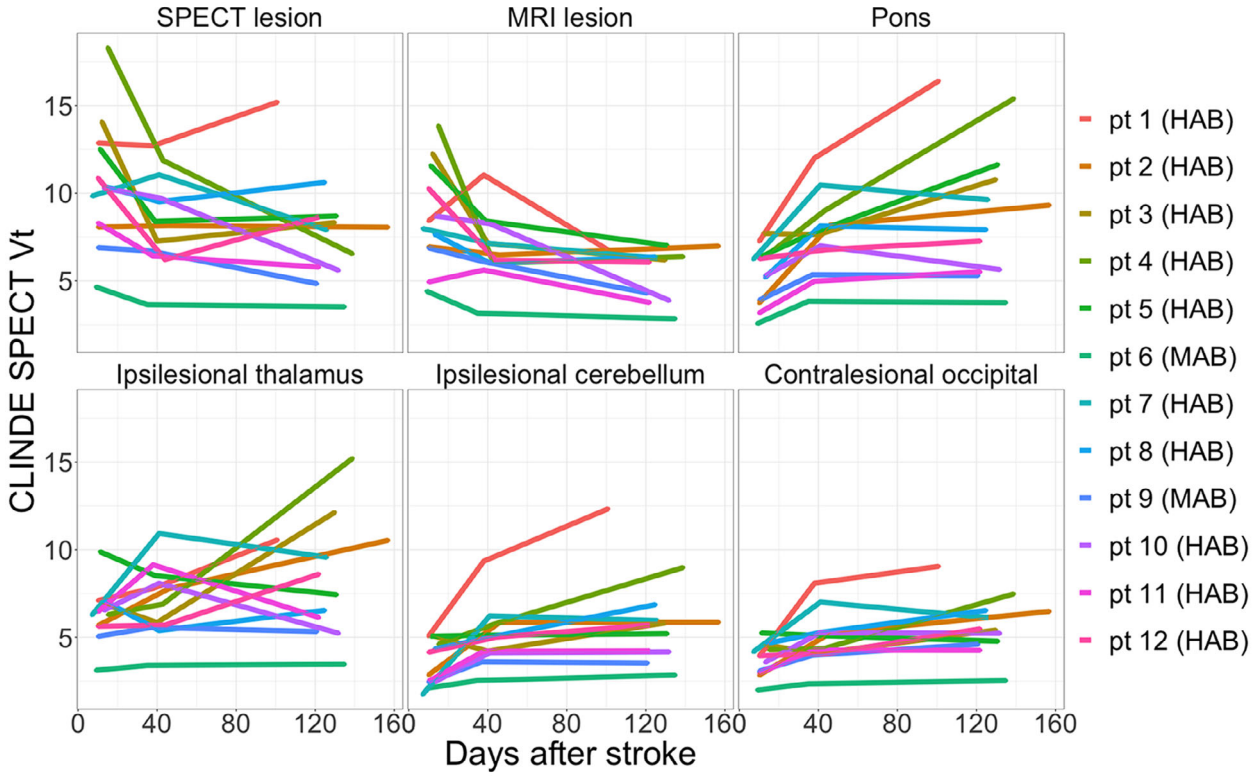

FIGURE 3 | Poststroke TSPO spaghetti plot. Spaghetti plots illustrating the individual longitudinal TSPO changes (CLINDE SPECT Vt) across various examined regions of interest for all patients included in the study. Vt, distribution volume; HAB, high-affinity binder; MAB, mixed-affinity binder; pt, patient.

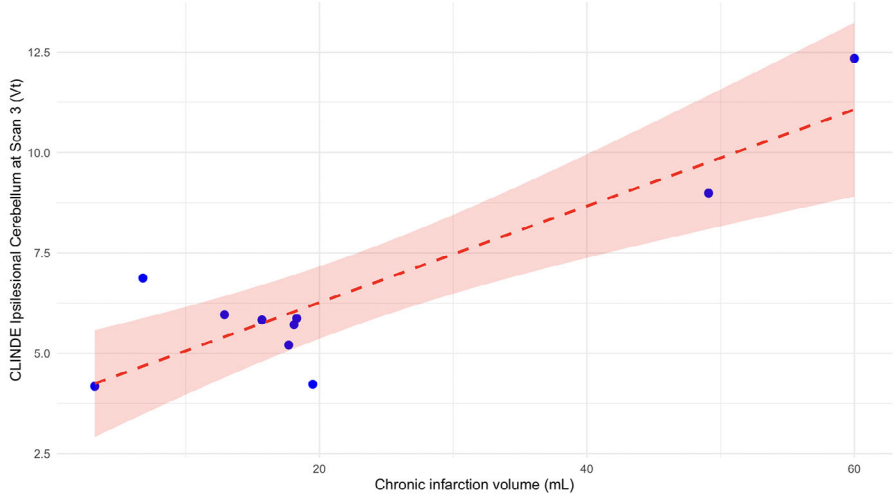

FIGURE 4 | Scatterplot of late-stage chronic infarction volume versus CLINDE SPECT Vt in ipsilesional cerebellum. The figure displays a scatterplot comparing the volume of chronic infarction delineated on FLAIR MRI at scan 3 to the CLINDE SPECT Vt in the ipsilesional cerebellum at scan 3. The plot also includes a linear regression line with 95% confidence intervals. Vt, distribution volume; FLAIR, fluid-attenuated inversion recovery.

the infarcted hemisphere at Days 13 and 20 [21]. A later study by Thiel et al. investigated a cohort of 18 stroke patients and six controls with transient ischemic attack. The study revealed a significant elevation in [11C]-PK11195 uptake ratio in an ellipsoid region positioned at the infarct site within 3 weeks following the stroke debut. Additionally, a significant longitudinal decrease was observed at the 6-month rescan [10].

TSPO expression surrounding the MRI lesion, commonly referred to as perilesional TSPO binding, as well as the partial overlap between lesional TSPO upregulation and the MRI lesion has been consistently observed [9, 22, 23]. This phenomenon has been investigated in a [11C]-PK11195 PET study in human stroke by Gerhardt et al., who demonstrated increased perilesional [11C]-PK11195 binding from Day 3 to Day 6 after stroke. Furthermore,

the PET-defined region increased in size and displayed a 46%–86.7% overlap with the infarct defined on T1-weighted MRI at Days 9–28 [8]. In our study, the first scan was performed between 7 and 15 days after stroke, and therefore, we did not investigate early TSPO upregulation. At the examined time period, a significant heterogeneity was observed between patients in terms of the initial overlap between the SPECT lesion ROI and the T2-weighted MRI lesion ROI (figure 1). Findings by Morris et al., in a study of 16 stroke patients, demonstrate that selective neuronal loss (SNL), assessed using ^{11}C-flumazenil, occurs in the penumbra with minimal TSPO expression, as measured by ^{11}C-PK11195. This suggests that microglial activity may not drive SNL [24]. These results are consistent with our findings, which demonstrate heterogeneity in the regional overlap between the SPECT and MRI lesional ROIs at Days 7–14. In some cases, the SPECT-defined ROI occupied only a portion of the lesion identified on T2-weighted MRI, while in others, it encompassed the majority of the lesion. A limitation of the current study is that the SPECT lesion ROI was defined using a cerebellar reference region at the first scan. At this stage we presume that the TSPO signal is unaffected by the stroke. However, our study found that TSPO increases in this region at the chronic stage after stroke, raising concerns about its viability as a reference region for such analyses. Since we did not examine acute changes in TSPO expression, it remains unclear whether TSPO in the ipsilateral cerebellum is affected by the stroke during the acute and early subacute phase. Further investigation is needed to determine if the ipsilesional cerebellum can reliably serve as a reference region at earlier stages after stroke.

Increasing TSPO expression was observed in connected ROIs, specifically in the pons, while no significant increase was noted in the ipsilesional thalamus. Thiel et al. previously demonstrated, in a study involving 12 stroke patients with strokes affecting the pyramidal tract, that increased TSPO binding in the ipsilesional pons occurred within 3 weeks after stroke onset and persisted for 6 months and found no significant change in TSPO expression between scans. However, there was a significant correlation between the initial TSPO uptake ratio in the pons and the extent of pyramidal tract damage determined by diffusion tensor imaging [10].

Pappata et al. have reported a significant TSPO increase in the ipsilesional thalamus of stroke patients scanned between 60 and 365 days after infarction [9]. Furthermore, Gerhard et al. observed TSPO expression extending from the lesional site to interconnected areas within the same hemisphere, as well as in the contralesional thalamus, in a patient who underwent scanning at two different time points, specifically 28 and 150 days poststroke [8]. Statistically significant longitudinal TSPO increases were not found within the ipsilesional thalamus in our study. This may be attributed to the circumstance that a subgroup of stroke patients had initial ischemic lesions in close proximity to the ipsilesional thalamus. Due to the spatial proximity, the initial perilesional TSPO increase and subsequent decrease could impact the accurate measurement of late TSPO increases in the ipsilesional thalamus.

Significant longitudinal increases in TSPO expression were observed in nonconnected regions, namely the ipsilesional cerebellum and the contralesional occipital cortex. Contralesional TSPO elevation has been reported in prior studies investigating stroke. Specifically, TSPO upregulation was observed in the contralateral hemisphere 30 days after stroke and in the contralesional thalamus at 150 days poststroke [8, 11]. A recent pilot study by D'Anna et al. showed that TSPO expression, as assessed with [11C]PBR28, is isolated to and resolves in the infarcted area as defined on MRI within 90 days poststroke [25]. The time course in the MRI-defined infarct is in line with our findings (Figure 2). However, regarding brain regions such as the occipital cortex and cerebellum, our data demonstrate significant TSPO increases, suggesting that these areas may not serve as stable reference regions for TSPO quantification at later time points. Conversely, other studies on TSPO imaging in stroke have employed presumed unaffected regions, such as the ipsilateral cerebellum or the unaffected hemisphere, as reference regions for quantifying the TSPO expression [10, 22, 26]. In addition, we demonstrated a positive correlation between the volume of chronic infarction and ^{123}I-CLINDE SPECT V_T in the ipsilesional cerebellum at 128 days poststroke.

The increasing TSPO expression we observed in nonconnected brain regions suggests a more complex neuroinflammatory process following stroke. Shi et al. discussed evidence from both animal models and human studies, indicating that stroke may trigger a widespread inflammatory response extending beyond the initial lesion, and proposed that this "global brain inflammation" involves various immune cell types, including microglia and astrocytes, potentially contributing to neurodegeneration [27]. This aligns with our findings of TSPO upregulation in nonconnected regions and emphasizes the importance of further investigating these processes. These findings emphasize the potential clinical value of TSPO as a biomarker for evaluating neuroinflammation during the chronic phase following stroke. Understanding the mechanisms underlying this inflammation could open new avenues for therapeutic strategies aimed at modulating brain inflammation after stroke particularly at the chronic stage.

Acknowledgments

We would like to thank Svitlana Olsen and Agnete Dyssegaard for their assistance in this research.

Conflicts of Interest

The authors declare no conflicts of interest.

References

1. H. Boutin and L. H. Pinborg, "TSPO Imaging in Stroke: From Animal Models to human Subjects," *Clinical and Translational Imaging* 3 (2015): 423–435.

2. A. Thiel and W.-D. Heiss, "Imaging of Microglia Activation in Stroke," *Stroke; A Journal of Cerebral Circulation* 42 (2010): 507–512.

3. Y. Nakagawa and K. Chiba, "Diversity and Plasticity of Microglial Cells in Psychiatric and Neurological Disorders," *Pharmacology & Therapeutics* 154 (2015): 21–35.

4. M. Prinz and J. Priller, "Microglia and Brain Macrophages in the Molecular Age: From Origin to Neuropsychiatric Disease," *Nature Reviews Neuroscience* 15 (2014): 300–312.

5. F. Mattner, A. Katsifis, M. Staykova, P. Ballantyne, and D. O. Willenborg, "Evaluation of a Radiolabelled Peripheral Benzodiazepine Receptor Ligand in the Central Nervous System Inflammation of Experimental Autoimmune Encephalomyelitis: A Possible Probe for Imaging Multiple Sclerosis," *European Journal of Nuclear Medicine and Molecular Imaging* 32 (2005): 557–563.

6. A. Gerhard, B. Neumaier, E. Elitok, et al., "In Vivo Imaging of Activated Microglia Using [11C]PK11195 and Positron Emission Tomography in Patients After Ischemic Stroke," *NeuroReport* 11 (2000): 2957–2960.

7. B. A. Radlinska, S. A. Ghinani, P. Lyon, et al., "Multimodal Microglia Imaging of Fiber Tracts in Acute Subcortical Stroke," *Annals of Neurology* 66 (2009): 825–832.

8. A. Gerhard, J. Schwarz, R. Myers, R. Wise, and R. B. Banati, "Evolution of Microglial Activation in Patients After Ischemic Stroke: A [11C](R)-PK11195 PET Study," *Neuroimage* 24 (2005): 591–595.

9. S. Pappata, M. Levasseur, R. N. Gunn, et al., "Thalamic Microglial Activation in Ischemic Stroke Detected in Vivo by PET and [11C]PK1195," *Neurology* 55 (2000): 1052–1054.

10. A. Thiel, B. A. Radlinska, C. Paquette, et al., "The Temporal Dynamics of Poststroke Neuroinflammation: A Longitudinal Diffusion Tensor Imaging-Guided PET Study With 11C-PK11195 in Acute Subcortical Stroke," *Journal of Nuclear Medicine* 51 (2010): 1404–1412.

11. C. J. S. Price, "Intrinsic Activated Microglia Map to the Peri-Infarct Zone in the Subacute Phase of Ischemic Stroke," *Stroke; A Journal of Cerebral Circulation* 37 (2006): 1749–1753.

12. L. Feng, C. Svarer, G. Thomsen, et al., "In Vivo Quantification of Cerebral Translocator Protein Binding in Humans Using 6-Chloro-2-(4'-123I-Iodophenyl)- 3-(N,N-Diethyl)-Imidazo[1,2-a]Pyridine-3-Acetamide SPECT," *Journal of Nuclear Medicine* 55 (2014): 1966–1972.

13. S. E. Ebert, P. Jensen, B. Ozenne, et al., "Molecular Imaging of Neuroinflammation in Patients After Mild Traumatic Brain Injury: A Longitudinal 123 I-CLINDE Single Photon Emission Computed Tomography Study," *European Journal of Neurology* 26 (2019): 1426–1432.

14. L. Airas, E. Rissanen, and J. O. Rinne, "Imaging Neuroinflammation in Multiple Sclerosis Using TSPO-PET," *Clinical and Translational Imaging* 3 (2015): 461–473.

15. D. R. Owen, A. J. Yeo, R. N. Gunn, et al., "An 18-kDa Translocator Protein (TSPO) Polymorphism Explains Differences in Binding Affinity of the PET Radioligand PBR28," *Journal of Cerebral Blood Flow and Metabolism* 32 (2012): 1–5.

16. P. Jensen, L. Feng, I. Law, et al., "TSPO Imaging in Glioblastoma Multiforme: A Direct Comparison Between 123ICLINDE-SPECT, 18F-FET PET and Gadolinium-Enhanced MRI," *Journal of Nuclear Medicine* 56 (2015): 1386–1390.

17. P. A. Yushkevich, J. Piven, H. C. Hazlett, et al., "User-Guided 3D Active Contour Segmentation of Anatomical Structures: Significantly Improved Efficiency and Reliability," *Neuroimage* 31 (2006): 1116–1128.

18. C. Svarer, K. Madsen, S. G. Hasselbalch, et al., "MR-Based Automatic Delineation of Volumes of Interest in Human Brain PET Images Using Probability Maps," *Neuroimage* 24 (2005): 969–979.

19. A. Dmitrienko and R. D'Agostino, "Traditional Multiplicity Adjustment Methods in Clinical Trials," *Statistics in Medicine* 32 (2013): 5172–5218.

20. P. Jensen, *Translocator Protein Imaging With 123I-CLINDE SPECT—Method Development and Clinical Research Copenhagen* (Copenhagen, Denmark: Eget forlag, 2017).

21. S. C. Ramsay, C. Weiller, R. Myers, et al., "Monitoring by PET of Macrophage Accumulation in Brain After Ischaemic Stroke," *The Lancet* 339 (1992): 1054–1055.

22. M.-J. Ribeiro, J. Vercouillie, S. Debiais, et al., "Could 18 F-DPA-714 PET Imaging be Interesting to Use in the Early Post-Stroke Period?," *EJNMMI Research* 4 (2014): 28.

23. B. Gulyas, M. Toth, A. Vas, E. Shchukin, J. Hillert, and C. Halldin, "Visualising Neuroinflammation in Post-Stroke Patients: A Comparative PET Study With the TSPO Molecular Imaging Biomarkers [^{11} C]PK11195 and [^{11} C]Vinpocetine," *Current Radiopharmaceuticals* 5 (2012): 19–28.

24. R. S. Morris, P. Simon Jones, J. A. Alawneh, et al., "Relationships Between Selective Neuronal Loss and Microglial Activation After Ischaemic Stroke in man," *Brain* 141 (2018): 2098–2111.

25. L. D'Anna, G. Searle, K. Harvey, P. M. Matthews, and R. Veltkamp, "Time Course of Neuroinflammation After Human Stroke—A Pilot Study Using Co-Registered PET and MRI," *BMC Neurology* 23 (2023): 193.

26. B. Gulyás, M. Tóth, M. Schain, et al., "Evolution of Microglial Activation in Ischaemic Core and Peri-Infarct Regions After Stroke: A PET Study With the TSPO Molecular Imaging Biomarker [11C]Vinpocetine," *Journal of the Neurological Sciences* 320 (2012): 110–117.

27. K. Shi, D.-C. Tian, Z.-G. Li, A. F. Ducruet, M. T. Lawton, and F.-D. Shi, "Global Brain Inflammation in Stroke," *Lancet Neurology* 18 (2019): 1058–1066.